Jun.2011／Vol.135

MITSUBISHI ELECTRIC
ADVANCE

Power Semiconductors Contribute to a Low−carbon Society

MITSUBISHI ELECTRIC
Changes for the Better

CONTENTS

Technical Reports

Overview

Author: *Kazuo Kyuma**

Power Devices for a Low-carbon Society

Power semiconductors are increasingly being used throughout the power electronics industry, including for general-purpose industrial machines such as inverters, robots and machine tools; home appliances such as air conditioners and washing machines; and social infrastructure such as electric railways and automotives (EV and HEV). Applications for power conversion equipment are also increasing, such as for uninterruptible power supplies, power conditioners for solar/wind power generators, and medical power supplies.

To create a low-carbon society, the development of advanced power electronic equipment is considered to be indispensable. Power semiconductors, which are essential for such equipment, must provide a solution for lower power consumption, along with better performance, smaller size, and greater functionality, as demanded by the application side.

Mitsubishi Electric has been developing high-performance power semiconductor devices for a wide range of applications including home electronic appliances, industrial machines, electric railways and automotives. For the Si chips that are at the heart of power semiconductors, we have introduced the Carrier Stored Trench Gate Bipolar Transistor (CSTBT) structure to reduce power loss and make the equipment smaller. We have also started to develop promising next-generation silicon carbide (SiC) devices, which are expected to revolutionize the power electronics industry. Meanwhile, we have developed various package structures ranging from transfer molds for low power-end inverter applications to case-type packages. To satisfy the various needs of customers, our broad product lineup includes the Insulated Gate Bipolar Transistor (IGBT) module and the Intelligent Power Module (IPM), which comes with a built-in circuit for performing dedicated drive and protection functionalities.

By developing various power semiconductor technologies for power chips, packages and drive circuits (including LVICs and HVICs), we will continue to offer high performance, compact, and supremely reliable power semiconductors, thus helping to create a low-carbon society.

As developing countries with large populations continue to grow, global energy demand is expected to surge. We firmly believe that power semiconductors are therefore essential to help convert energy efficiently and reduce energy consumption.

*Representative Executive Officer, Executive Vice President
  In charge of Semiconductor & Device

SiC Power Device Technology

Authors: *Shuhei Nakata*, Naruhisa Miura** and *Yoshiyuki Nakaki**

Silicon carbide (SiC) is expected to provide an energy-saving power converter. This paper describes the development, application and future outlook for the SiC type high-capacity, low-loss power devices of the Metal Oxide Semiconductor Field Effect Transistor (MOSFET) and Schottky Barrier Diode (SBD), which we used to create a power converter with significantly reduced power loss (by 70% from conventional level).

1. Introduction

SiC offers advantages as a semiconductor material over conventional Si, including dielectric breakdown field strength that is about one order of magnitude higher than that of Si.

Because of this high dielectric breakdown field strength, SiC can be used to design high-voltage unipolar devices, which is not possible with Si. Such SiC unipolar devices can greatly reduce the conduction loss as well as the switching loss (when turned on/off). Therefore, by using SiC devices for the inverters in power conversion devices, the power loss as well as the equipment size can be significantly reduced.

Mitsubishi Electric has been concurrently developing SiC devices, including SiC-MOSFET and SiC-SBD, with better basic performance, and inverters and other technologies for practical application of SiC devices.

In January 2006, Mitsubishi developed 10-ampere-class SiC devices having a withstand voltage of 1200 V (SiC-MOSFET and SiC-SBD) and for the first time in the world, successfully operated an SiC inverter using these devices to drive a 3.7-kW rated three-phase motor. In October 2007, we used a prototype 3.7-kW inverter to demonstrate that for low-loss characteristics, the equipment volume can be reduced to a quarter of the conventional volume (power density of 10 W/cm^3) [1].

In February 2009, we achieved an output power of 10 kW by combining modules consisting of parallel-connected 10A-class SiC devices, and demonstrated that the power loss could be reduced by 70% from that of the conventional Si inverter. [2]

This paper describes the development of high-capacity SiC devices and their application to an 11-kW inverter.

2. Development of SiC Devices

2.1 SiC-MOSFET

The SiC-MOSFET under development is a so-called vertical-type MOSFET having a structure as shown in the upper part of Fig. 1. Explanation of the structure is as follows. The substrate is an n-type SiC wafer, on which an epitaxially grown drift layer is formed. The thickness and the effective impurity concentration in the drift layer are designed so that the leak current remains sufficiently low when the rated voltage is applied to the drain electrode.

The drain current–voltage characteristics of this SiC-MOSFET device at room temperature are shown in the lower part of Fig. 1. The effective chip area is about 0.2 cm^2, and as shown, the MOSFET can control the drain current up to 100 A.
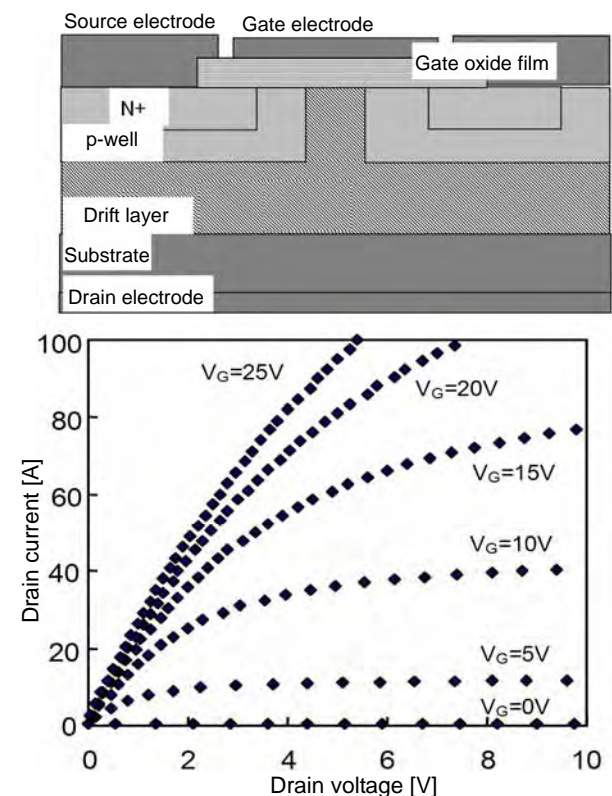

Fig. 1 Structure of MOSFET and electrical characteristics

2.2 SiC-SBD

Similarly to the MOSFET, SiC-SBD is also fabricated using an n-type SiC wafer. The thickness and the impurity concentration in the drift layer are designed in the same manner as in the case of the SiC-MOSFET so

that the leak current remains sufficiently low when the rated voltage is applied.

Figure 2 shows the current–voltage characteristics of the fabricated prototype SiC-SBD at room temperature. The chip size is about 5 mm square and the effective chip area is about 0.25 cm^2. As shown, a current begins to flow at a forward voltage of 0.96 V (V_{th}), and then the current–voltage characteristic becomes typical for the SBD.
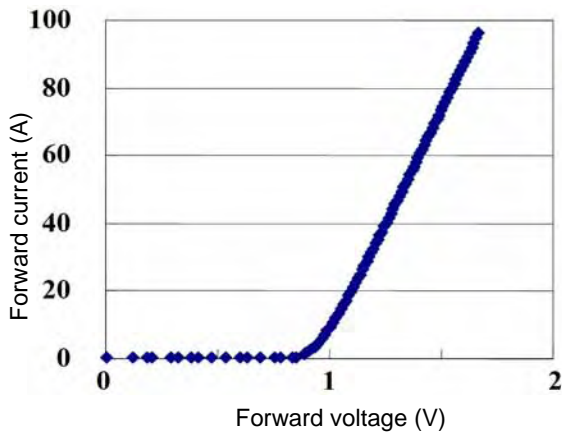

Fig. 2 Electric characteristics of SBD

3. Fabrication and Evaluation of Prototype 11-kW SiC Inverter

3.1 11-kW SiC Inverter

Using the SiC devices described in the previous section, we fabricated a prototype high-power inverter. The results are as follows.

Figure 3 shows the arrangement of the chips inside the module. This module is the building block of the prototype inverter and each module consists of a converter, inverter and brake circuits. In the photo, the left part is the converter circuit and the right part is the inverter and brake circuits. The converter consists of Si diodes, and the inverter and brake circuits are constructed with SiC-MOSFETs and SiC-SBDs. The chips circled by dashed lines and dotted lines are SBDs and MOSFETs, respectively.
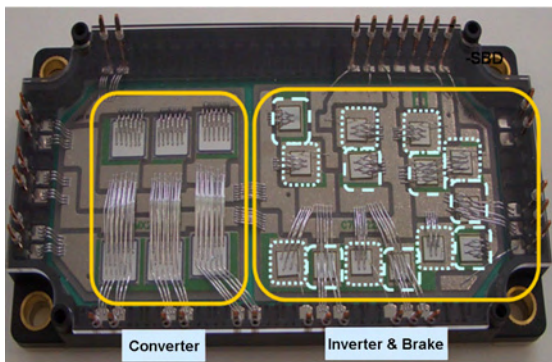

Fig. 3 SiC device layout in the fabricated SiC inverter

The evaluation results of the dynamic characteristics (switching waveforms) of the SiC inverter are shown in Fig. 4. The measurement was carried out through the upper and lower arms of the module by using an inductive load. The waveforms shown were measured at 125°C.

Figure 4 shows the current and voltage waveforms obtained when the power is turned on (upper chart) or turned off (lower chart). The dark and light lines indicate the waveforms of the SiC device and the conventional Si device, respectively.
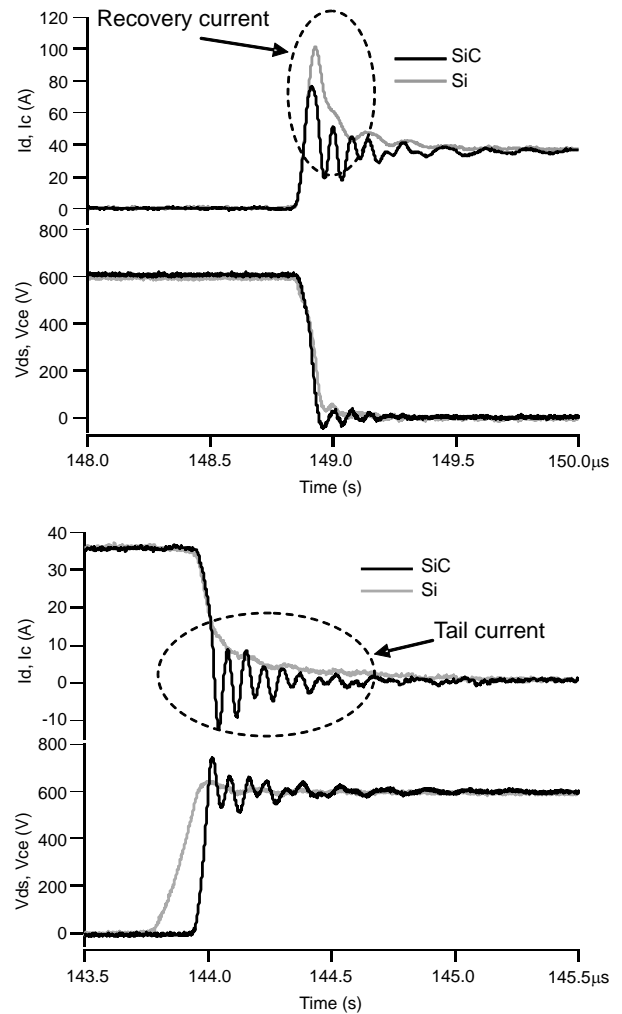
Fig. 4 Switching waveform of the inverter

When the power is turned on (upper chart), the SiC device exhibits a lower spiking current (recovery current) than the Si device does. This result is an effect of the SBDs, and the oscillation observed in the waveform occurs because of the parasitic capacitance and inductance in the circuit.

When the power is turned off (lower chart), a tail current appears in the waveform of the Si device, whereas the SiC device promptly shuts off the power.

For inverter operation (carrier frequency: 15 kHz, power factor: 0.8, effective current: 23 A, power output:

11 kW), the power loss is calculated using the relationship between the current value and the switching loss obtained from the switching test above, along with the measurements of the static characteristics (I–V characteristics).

Figure 5 shows the calculated power loss for the Si device and SiC device. As shown, overall power loss is greatly reduced by 70% from that of the conventional Si inverter. Figure 5 also shows the respective conduction and switching (SW) losses, indicating that the SiC device exhibits a dramatic reduction in the switching loss, which measures to 83% lower than that of the Si device.
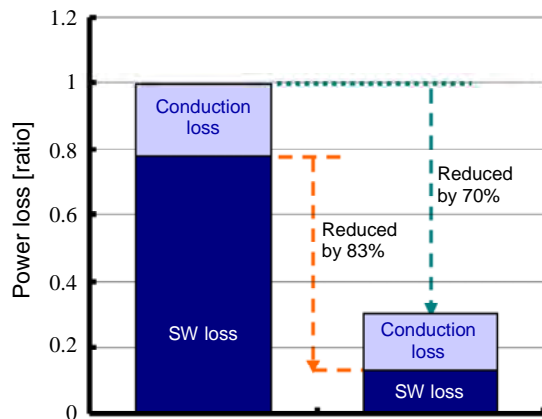

Fig. 5 Comparison of electrical power loss between a Si-inverter and the SiC-inverter

3.2 Characteristics of SiC Inverter

A lower inverter loss means that the equipment can be made smaller. Figure 6 shows the prototype SiC inverter and its current and voltage waveforms obtained when controlling a motor (11 kW output) [4]. Because of the reduced power loss, a smaller cooling system is sufficient, and thus the volume of the SiC inverter is reduced to 1.1 L (1/4 of conventional inverter). As a result, a power density of 10 W/cm^3 has been achieved, which is about four times greater than that of the Si inverter with the same current capacity.

The lower part of Fig. 6 shows the current and voltage waveforms for controlling a motor at a power output of 11 kW. As clearly shown, the motor is controlled in a stable condition.

We have thus demonstrated that SiC devices use far less power than conventional inverters do, and that the inverter volume can be reduced to one quarter, thanks to the low loss, increasing the power density to 10 W/cm^3. We will continue to develop technologies for applying SiC devices to power conversion equipment toward early commercialization.

A part of this research project is the outcome of the "Development of Basic Technologies for Power Electronics Inverters" commissioned by the Ministry of Economy, Trade and Industry and NEDO.
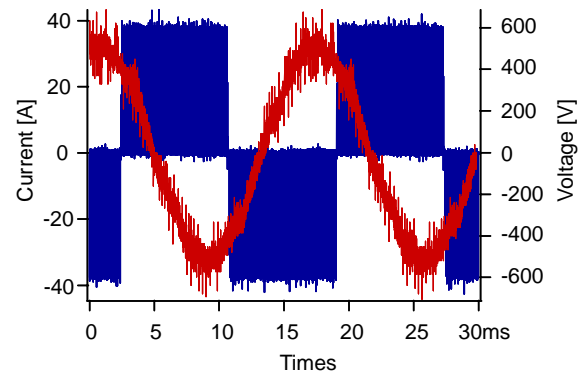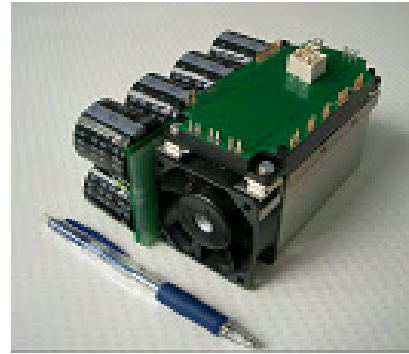
Fig. 6 The fabricated inverter and the waveform at PWM operation

References

(1) T. Watanabe, et al.: "Shuttle Activation Annealing of Implanted Al in 4H-SiC," Jpn. J. Appl. Phys. 47(4) 2841–2844 (2008).
(2) S. Kinouchi, et al.: "High Power Density SiC Converter," Material Science Forum Vols. 600–603, 1223–1226 (2009).
(3) S. Nakata, et al.: "Substantial Reduction of Power Loss in a 14 kVA Inverter Using Paralleled SiC-MOSFETs and SiC-SBDs," Silicon Carbide and Related Materials 2008, 903–906 (2009).
(4) S. Kinouchi and S. Nakata: "Energy Conservation and Resource Saving by SiC Inverter," Mitsubishi Denki Giho 83, No. 10, 27–30 (2009).

The 6th-Generation IGBT & Thin Wafer Diode for New Power Modules

Authors: *Tetsuo Takahashi** and *Yasuhiro Yoshiura**

1. Introduction

Power devices are becoming increasingly important for protection of the global environment. In addition to applications for industrial equipment such as conventional inverters and servos, and home appliances such as air conditioners and refrigerators, applications are expanding to hybrid cars, electric vehicles, wind power generation and solar power generation.

The main power devices used today are the Insulated Gate Bipolar Transistor (IGBT) and Free Wheeling Diode (FWD), and so improving their performance is crucial for the growth of power electronics. Since the late 1980s, Mitsubishi Electric has continually improved the performance of these devices by developing fine patterning processes, introducing low-loss IGBT such as CSTBT™, and other measures. As a result, the figure of merit (FOM) has been improved by ten folds since 2007.

This paper describes the development of even higher performance 6th-generation IGBTs and thin wafer diodes.

2. The 6th-Generation IGBT

2.1 Performance Improvement of IGBT

Since the first-generation IGBT was released in 1987, their performance has risen steadily, as shown by the figure of merit (FOM) improvement history in Fig. 1.

The FOM quantifies the device characteristics and is defined as:

$$FOM = \frac{J_C}{V_{CE(sat)} \times E_{OFF}} \qquad \text{........ Eq. (1)}$$

where, J_C (A/cm²) is the collector current density which primarily determines the chip size; $V_{CE(sat)}$ is the collector-emitter saturation which determines the stationary loss; and E_{OFF} (mJ/p/A) is the turn-off loss.

The first-generation IGBT was a planar type, and the performance has been steadily improved through the generations by fine patterning of the transistor cell. From the 4th generation, the planar structure was replaced by the trench type, which greatly improved the performance. The 5th-generation improved the performance by adopting the new IGBT structure called CSTBT and the thin wafer process.
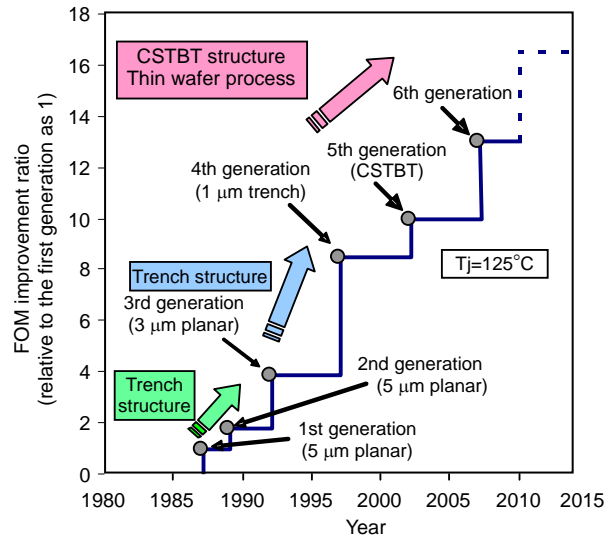

Fig. 1 Improvement of figure of merit (FOM) of IGBTs

2.2 Structural Features of the 6th-Generation IGBT

To achieve stable operation and improve performance, the 6th-generation IGBT uses: (1) high-energy implantation technology to form the impurity profile, (2) thin wafer process, and (3) fine patterning process with optimized cell structure.

Table 1 compares the 5th- and 6th-generation 1200 V-class IGBT structures.

Table 1 Comparison of the structures of 5th- and 6th-generation IGBTs

Structure / Item	5th generation	6th generation
Impurity profile	Standard	Retrograde
Thin wafer process	Applied	Applied
Trench pitch	Wide pitch	Narrow pitch
Cell structure	Standard	Optimized

To improve the uniformity of gate-emitter threshold voltage $V_{GE(th)}$, which is an important parameter of IGBT performance, the 6th-generation IGBT uses high-energy implantation technology to form the Carrier Stored (CS) layer by accelerating and implanting impurities by using a high electric field (retrograde).

Figure 2 shows the impurity profiles formed by the high-energy implantation technology. $V_{GE(th)}$ is primarily determined by the thickness of the MOS gate oxide film and the impurity concentration in the channel doped layer. For the 5th- and later generation IGBT, the CS

layer is additionally formed to optimize the carrier distribution in the n^- drift layer during conductivity modulation. For the 5th-generation IGBT, the CS layer is formed by thermal diffusion from the surface, and thus the impurity concentration in the region that governs the $V_{GE(th)}$ is determined by two diffusion processes: diffusion in the channel doped layer and diffusion in the CS layer. To minimize any problem that may cause variance in $V_{GE(th)}$, the 6th-generation IGBT uses implanting technology to inject high-energy impurities to form the CS layer. As a result, uniform $V_{GE(th)}$ has been achieved while maintaining the desired effect of the CS layer.

In addition, by further refining the thin wafer process used for the 5th-generation IGBT, the trade-off relationship between $V_{CE(sat)}$ and E_{OFF} has been improved. The cell structure parameters including the trench pitch have also been optimized to reduce the electro magnetic interference (EMI) noise and gate capacitance.

(a) Impurity profile in the 5th-generation IGBT

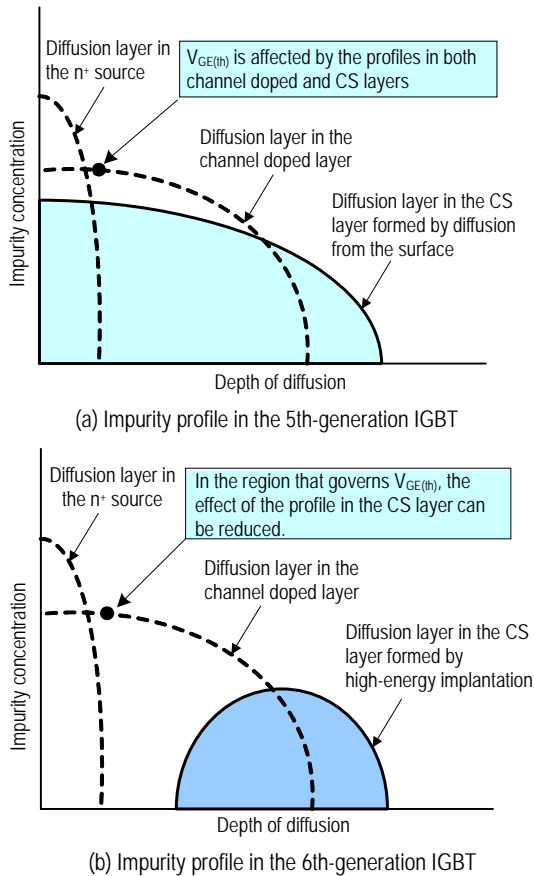(b) Impurity profile in the 6th-generation IGBT

Fig. 2 Impurity profile formed by high-energy implantation technology

2.3 Electric Characteristics of the 6th-Generation IGBT

Figure 3 shows the trade-off relationship between E_{OFF} and $V_{CE(sat)}$ for the 6th-generation IGBT and 5th-generation IGBT both rated as 150 A and 1200 V. Generally, an IGBT has a trade-off relationship between E_{OFF} and $V_{CE(sat)}$ and so a structure that improves this

trade-off is required. Compared with the 5th-generation IGBT, in the 6th-generation IGBT the $V_{CE(sat)}$ ratio is about 23% less and the FOM is improved by 31% (Fig. 1).
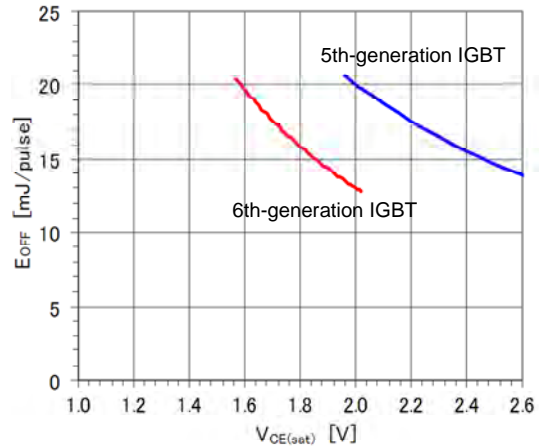

Fig. 3 Trade-off relationship between E_{OFF} and $V_{CE(sat)}$

3. Thin Wafer Diode

3.1 Structural Features of Thin Wafer Diode

The cathode layer of a conventional diode is formed by diffusing n-type impurities from the back surface. As a result, the cathode layer formed in the back surface becomes very thick, making it difficult to reduce the forward voltage drop V_F.

We greatly reduced the V_F of the thin wafer diode by applying the thin wafer process to the IGBT and redesigning the cathode profile.

3.2 Electric Characteristics of Thin Wafer Diode

Figure 4 shows the trade-off relationship between V_F and the recovery loss E_{rr} for the conventional and thin wafer type diodes. Generally, there is a trade-off relationship between V_F and E_{rr}, and improving this trade-off relationship is one of the keys in developing the diode. The thin wafer diode features a greatly improved V_F-E_{rr} trade-off, with a 33% lower E_{rr} at the same V_F.
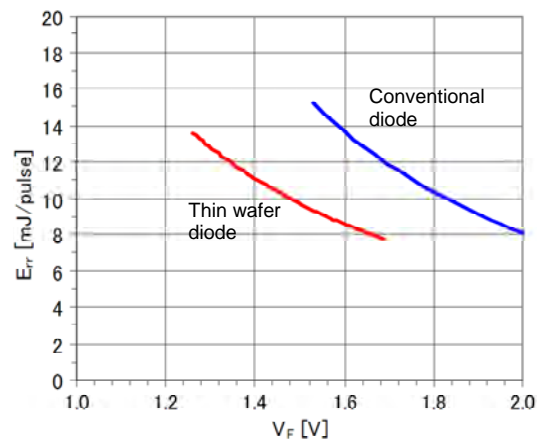

Fig. 4 Trade-off relationship between V_F and E_{rr}

The performance of the thin wafer diode is about 38% better than that of the conventional diode by using the following FOM:

$$FOM = \frac{J_A}{V_F \times E_{rr}} \qquad \text{........ Eq. (2)}$$

where, J_A is the anode current density (A/cm^2), V_F is the forward voltage drop (V) at 125°C, and E_{rr} is the recovery loss (mJ/A/pulse) at 125°C.

4. Conclusion

To develop a new type of low-loss, low-noise power module, we have developed a 1200 V-class 6th-generation IGBT and thin wafer type FWD. The FOMs of the IGBT and FWD are improved by 31% and 38%, respectively, thus meeting expectations for next-generation devices.

We also applied the developed technologies to 1700 V-class devices, and confirmed significant improvement over the 5th-generation devices. We plan to commercialize various products in turn. We will continue to improve the performance of Si devices and help expand power electronics to create an energy-saving society.

References

(1) Takahashi T., Tomomatsu Y., Sato K.: "CSTBT^{TM} (III) as the next generation IGBT," Proceedings of ISPSD 2008, 72–75 (2008).
(2) Sato K., Takahashi T., Fujii H., Yoshino M., John F Donlon: "New chip design technology for next generation power module," Proceedings of PCIM 2008, 673–678 (2008).
(3) Takahashi H., Haruguchi H., Hagino H., Yamada T.: "Carrier Stored Trench-Gate Bipolar Transistor (CSTBT) - A Novel Power Device for High Voltage Application," ISPSD '96, 349–352 (1996).
(4) Nakamura K., Kusunoki S., Nakamura H., Ishimura Y., Tomomatsu Y., Minato T.: "Advanced Wide Cell Pitch CSTBTs Having Light Punch-Through (LPT) Structures," ISPSD '02, 277–280 (2002).

R-Series HVIPMs

Authors: *Hitoshi Uemura* and Ryosuke Nakagawa***

As environmental issues have attracted increasing worldwide attention in recent years, electric railways with low CO_2 emissions are playing a key role. The railway industry expects the High Voltage Insulated Gate Bipolar Transistor (HVIGBT) to exhibit not only high reliability but also low power loss, high rated current, and high operating temperature.

Mitsubishi Electric pioneered the development of a High Voltage Intelligent Power Module (HVIPM), which consists of HVIGBTs with a built-in drive circuit and protective functions. The HVIPM has a large power capacity and can be used in power conversion equipment for railway vehicles. Since the HVIPM was first used for traction control in 1997, Mitsubishi Electric has been awarded many projects. We have therefore now developed the R-Series HVIPMs having a dielectric strength of 3.3 kV/ 6.5 kV and 25% higher rated current than conventional products.

This paper presents the features and evaluation results of the R-Series HVIPM which satisfies the performance requirements, focusing on the electrical characteristics of the 3.3-kV model.

1. Features of 3.3-kV R-Series HVIPM

The R-Series HVIPM has been developed on the basis of the following design concepts:

(1) Reduction of power loss: New IGBT and diode chips have been developed to reduce the power losses.

(2) Expanded operating temperature range: New structures of IGBT and diode chips have been adopted and the packaging material has been modified to achieve high operating temperatures up to 150°C as well as the minimum operating temperature of −50°C.

(3) Increased rated current: The rated current has been increased by 25% compared to the conventional HVIPM.

(4) Improved protective functions: A function to detect current and temperature has been built into the IGBT chip, which, in combination with the ACIC mounted on the control board, ensures high-accuracy protection.

(5) High reliability: Since electric railways require high reliability, sufficient Safe Operating Area (SOA) capability has been secured. In addition, the optimized package structure offers improved reliability.

2. R-Series IGBT Chip

As shown in Fig. 1, the structure of the IGBT chip has been modified from the conventional Punch Through (PT) to the Light Punch Through (LPT) type, thus reducing the turn-on voltage (V_{CEsat}) by optimizing the cell structure. In addition, as shown in Fig. 2, the output current exhibits negative feedback characteristics, that is, "as the temperature rises, the current decreases." This maintains a stable current balance be-
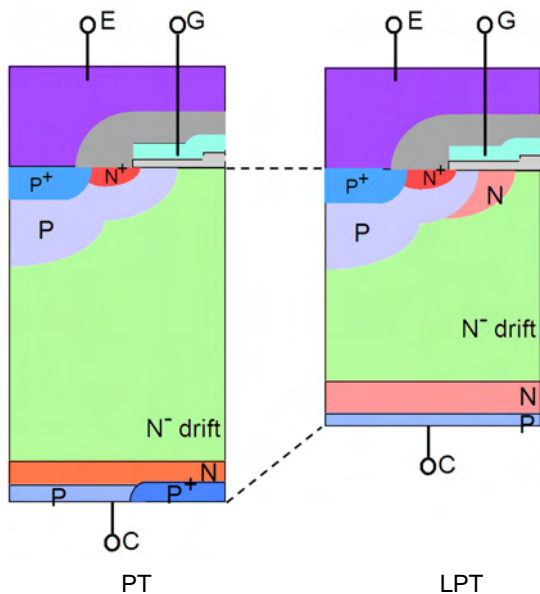

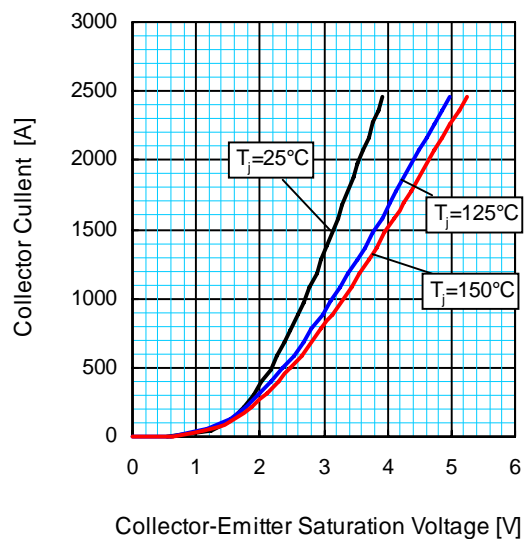Fig. 1 Comparison of conventional PT and LPT IGBT chips

Fig. 2 Ic-V$_{CE}$ characteristics of Rseries HVIPM

*Power Device Works **Itami Works

tween IGBT chips, making it easy to operate multiple IGBTs connected in parallel. Figure 3 shows the trade-off curve between V_{CEsat} and E_{off}, which indicates that the R-Series HVIPM achieves a 25% lower V_{CEsat} at the same E_{off} compared to the conventional HVIPM.
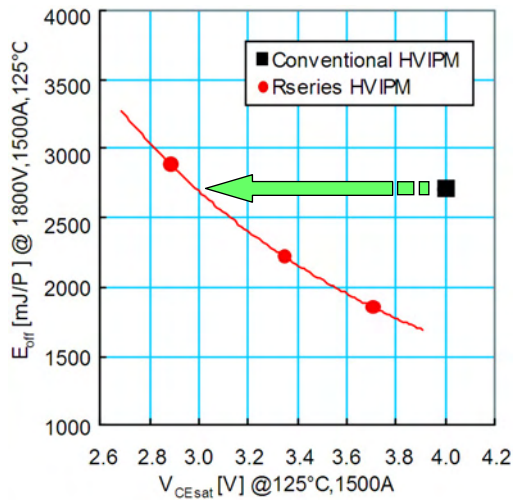

Fig. 3 Comparison of Eoff-V_{CEsat} characteristics of conventional HVIPM and Rseries HVIPM

3. Expanded Operating Temperature Range

The operating temperature of the conventional HVIPM is restricted to −40°C to +125°C due to the limitations of the constituent materials and the thermal breakdown caused by increased power loss in the IGBT and diode chips. High operating temperatures are now made possible thanks to the new IGBT and diode structures, thus reducing the power loss. Meanwhile, one of the constituent materials that limit the temperature range is the filling material (silicone gel) used to ensure insulation, so in cooperation with the material manufacturer, Mitsubishi Electric has developed a new filling material with greatly improved thermal characteristics. With these improvements, the operating temperature range has been expanded to −50°C to +150°C, enabling a higher system output and greater freedom for designing the cooling system.

4. Increased Rated Current

The maximum rated current of the R-Series HVIPM with a dielectric strength of 3.3 kV has been increased to 1500 A, a 25% improvement from the conventional 1200 A. As an example, the inverter output current is calculated with respect to the carrier frequency f_c as shown in Fig. 4. A comparison made at T_{jmax} = 125°C indicates that the inverter's output current can be increased by 250 A (about 25%) at f_c = 500 Hz; and at T_j = 150°C, it can be increased by about 550 A (about 55%). To cope with the heat generated by the main electrode resulting from the increased current, the design of internal wiring was optimized to reduce the

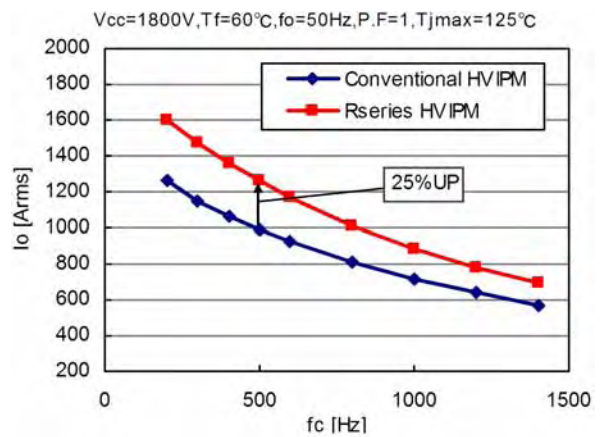wiring resistance by 50% compared with the conventional model.

Fig. 4 Output current of inverter

5. High-Accuracy Protective Function

Mitsubishi Electric's HVIPM is equipped with protective functions (Under Supply Voltage (UV), Over-Current (OC), and Over-Temperature (OT)), and by improving the accuracy of these protective functions and reducing inter-component variance, an excessively wide margin in the design of power conversion equipment is no longer needed, and thus an economic and high-performance system design is possible.

Electric railways involve frequent acceleration/deceleration and a wide range of load capacity, train occupancy and changes in gradient. Therefore, instantaneous over-current and abrupt temperature changes need to be considered, and in case of abnormality, the protective function must operate immediately.

The R-Series HVIPM has a current detection sensor built into the IGBT chip, which is used in combination with the dedicated IC to realize a more accurate over-current protection circuit than the previous model.

Similar to the current sensor, a temperature sensor is also built into the IGBT chip. Figure 5 shows an in-plane temperature distribution of the R-Series HVIPM and the accuracy of temperature measurement by the temperature sensor. A comparison between the surface temperatures measured by an IR camera and those estimated by the temperature sensor shows that, over any temperature range, the temperature of the chip is accurately detected. In addition, by using this function in combination with the dedicated IC mounted on the control board, high-accuracy over-temperature protection with improved responsiveness has been realized.

6. Higher SOA Capability

The HVIPM requires excellent reliability such as a sufficiently high SOA capability. Figure 6 shows the type test results of the R-Series HVIPM for the turn-off and reverse recovery operations at the maximum junction temperature of 150°C. The turn-off waveforms indicate

no abnormalities and stable operation is confirmed even under test conditions exceeding the limit of SOA.

The new diode chip was designed to perform soft recovery operation; and the reverse recovery waveforms indicate that the new design successfully suppresses oscillations during the recovery period, resulting in improved SOA capability. The marginal test confirmed that the peak loss (P_{rr}), which is an indicator of the SOA capability, has a margin of three times the specification.
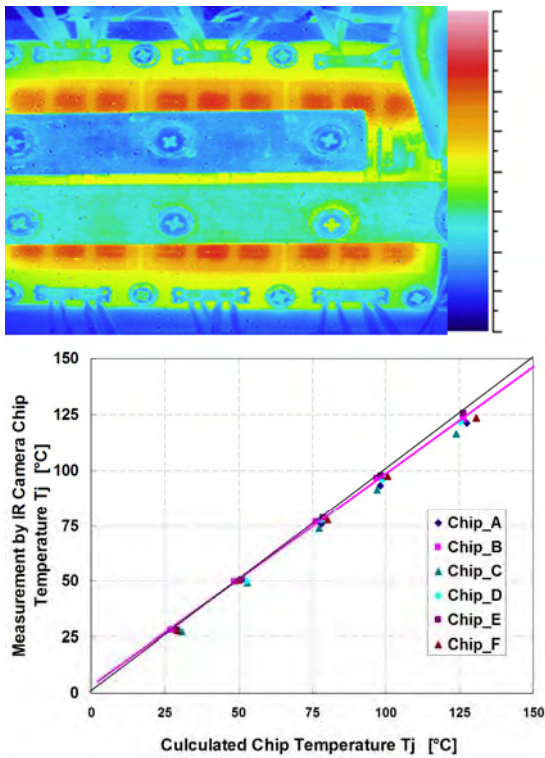
7. Package Compatibility

Figure 7 shows an external view of the R-Series HVIPM; the conventional external dimensions, electrode arrangement and signal interface are the same but the internal structure is improved, allowing easy upgrading from the existing system.

We will continue to develop products that reflect diverse customer needs, and provide high performance, high reliability products.

Fig. 5 Chip temperature measurement result and the detection precision of the thermal sensor
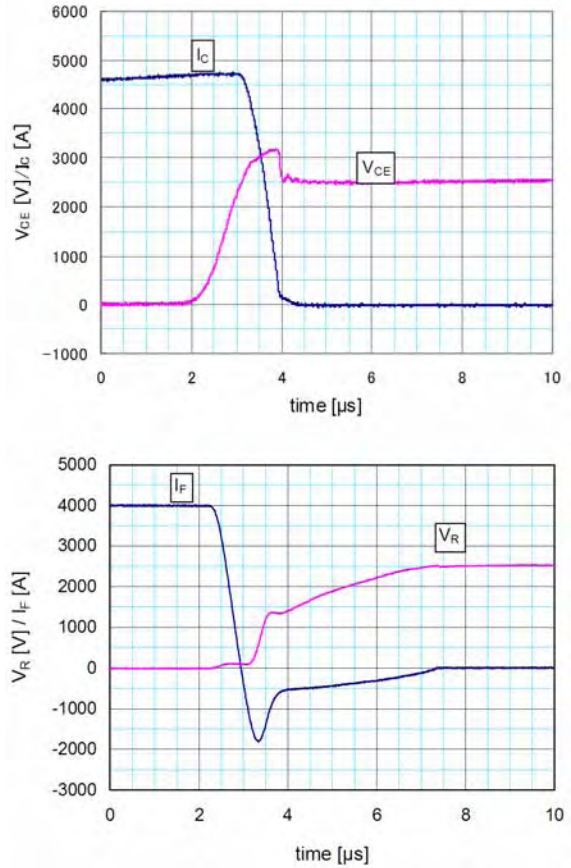

Fig. 6 Turn-off and reverse waveforms of the type test result

a. 3.3kV R series HVIPM

b. 6.5kV R series HVIPM

Fig. 7 The R series HVIPMs

References
(1) S. Iura et al.: "Development of New Generation 3.3 kV IGBT module," PCIM Europe 2006 (2006).
(2) T. Kobayashi et al.: "Trend of Power Device for Railway Vehicles," Mitsubishi Giho, 83, No. 11, 657–659 (2009).
(3) T. Kobayashi et al.: "Trend of Power Device for Railway Vehicles," Proceedings of the 46th Railway Cybernetics Symposium, 513 (2009).

New High-Power 2-in-1 IPM "V1 Series"

Authors: *Nobuya Nishida* and Shiori Uota**

Many countries are striving to save energy and so IPMs are now used in a wide range of applications, yet there is a growing need for further loss reduction, higher capacity, and longer lifetime. To meet these needs, we have released the high-power 2-in-1 IPM "V1 Series." This article presents the features and component technologies of the V1 Series.

1. Introduction

It is now 13 years since the Kyoto Protocol was signed. Energy saving is a challenge for all countries in order to protect the global environment, and the Intelligent Power Module (IPM) is a key tool to help solve the challenge.

IPMs are not only used for servos and inverters that have long been in demand, but are now also being used for various other fields including clean energy and construction machinery. Accordingly, there is a growing need for loss reduction as well as higher capacity and longer lifetime.

To meet these market needs, we have released the high-power 2-in-1 IPM V1 Series with the following features:

(1) The 2-in-1 circuit configuration and full product lineup in the high capacity range allow easy use in various applications.
(2) For easy upgrading from the old-generation 2-in-1 V Series, the V1 Series has the same dimensions and terminal configuration as the old series.
(3) The IPM's inner configuration has been thermally designed to improve the heat dissipation, and so a high capacity (large current) has been achieved with the same external dimensions as the V Series.
(4) By optimizing the circuit design, over-current at the time of a load short circuit is suppressed, resulting in an improved short-circuit safe operating area (SOA)

in comparison with the old-generation products.
(5) By optimizing the wire bonding conditions for the electrical connections inside the IPM, the ΔT_j of the V1 Series after 1000k power cycles is improved to $\Delta 60°C$ from $\Delta 32°C$ and $\Delta 45°C$ of the old-generation V Series and L Series, respectively.
(6) By operating parallel-connected chips of 0.8 μm full-gate Carrier Stored Trench-gate Bipolar Transistor (CSTBT), which were also used by the prior L1 Series (6-in-1 and 7-in-1), the current capacity is increased and the power loss is reduced by 21% and 23% from the old-generation V Series and L Series, respectively.

2. Product Lineup

Many countries are striving to save energy and so IPMs are now used in a wide range of applications, yet there is a growing need for further loss reduction, higher capacity, and longer lifetime.

To meet these needs, we have developed the new high-power 2-in-1 IPM V1 Series, with the product lineup as listed in Table 1.

For easy upgrading from the old-generation V Series, the V1 Series has a full product lineup in the high capacity range, and even has the same external dimensions and pin configuration as the V Series.

The V1 Series has an improved power cycle lifetime comared to the old-generation products, and also has a reduced power loss thanks to the 5th-generation full-gate CSTBT chips which have been inherited from the prior L1 Series. Thus, the V1 Series products meet the market needs.

3. Component Technologies

This section describes the component technologies that characterize the V1 Series.

Fig. 1 Visual of the high power 2inl IPM "V2 series"

3.1 Power Device (Technology for loss reduction)

The old-generation V Series were equipped with planar type Insulated Gate Bipolar Transistor (IGBT), whereas the L Series were equipped with Plugging Cell Merged (PCM) CSTBTs that control the channel density (Fig. 2).

Compared to the planar type IGBT, the PCM CSTBT has a similar gate charge and short-circuit SOA, but a lower loss. Therefore, the old-generation L Series adopted the PCM structure.

In order to meet the requirement for a further reduction in loss, the V1 Series has adopted the full-gate CSTBT, the low-loss version of the PCM structure, in the same manner as the prior L1 Series (Fig. 3).

Figure 4 compares the results of power loss simulations for the V1 Series and the old-generation V Series and L Series. With the full-gate CSTBT, the V1 Series has reduced the total power loss by 21% and 23% from the old-generation V Series and L Series, respectively.

The simulation was performed under the following conditions:

PN voltage V_{cc} = 600 V, carrier frequency f_c = 15 kHz, IPM output current I_o = 1800 A_{peak}, power factor PF = 0.8, modulation factor = 1, and junction temperature T_j = 125°C.

(Note) Since the L Series has the 6-in-1 configuration, the calculation was performed for the 1/3 module (consistency of comparison conditions)

3.2 Control (Improvement of Short-Circuit SOA)

In addition to the reduction of power loss, the V1 Series has achieved a high current capacity by operating parallel-connected full-gate CSTBT chips.

When operating multiple chips in parallel, there is a risk of gate oscillation, current imbalance between chips, or associated over-current due to load short-circuit, which would result in a deteriorated short-circuit SOA capability compared with the old-generation products.

To solve this problem, the pattern and circuit designs have been optimized for the V1 Series, resulting in successful operation of parallel-connected full-gate CSTBT chips as well as improved short-circuit SOA capability. As a result, the power loss is reduced and the current capacity is increased in comparison with the old-generation products.

Figure 5 shows the current waveform of the V1 Series during a load short circuit. When the short-circuit occurs, an excessive peak current of about 6,000 A occurs with the conventional design, whereas the V1 Series exhibits improved protection of the IGBT and the peak current is suppressed by 42%.

3.3 Thermal Design (Technology for Capacity Enhancement)

In the structural design of the V1 Series IPM, thermal simulations were performed on the thermal interference in the power output part and the wire bonding area to improve the heat dissipation over the

Table 1 Products lineup of V1 series IPM

| Voltage rating	Current rating	V1 series		(Ref.) V series	
		Type name	Package	Type name	Package
600V	400A	PM400DV1A060	small PKG	PM400DVA060	small PKG
	600A	PM600DV1A060	small PKG	PM600DVA060	large PKG
	800A	PM800DV1A060	large PKG	-	-
1200V	200A	PM200DV1A120	small PKG	PM200DVA120	small PKG
	300A	PM300DV1A120	small PKG	PM300DVA120	large PKG
	450A	PM450DV1A120	small PKG	-	-
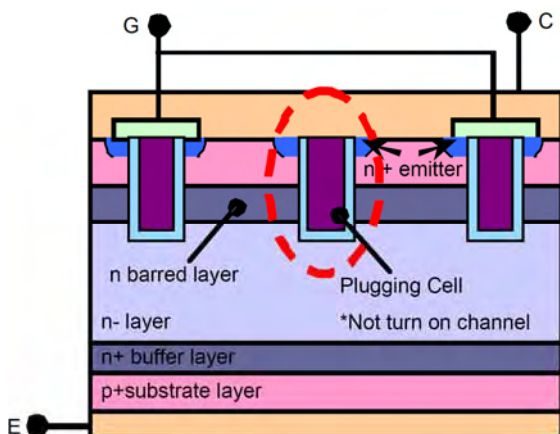
Fig. 2 Structure of PCM CSTBT
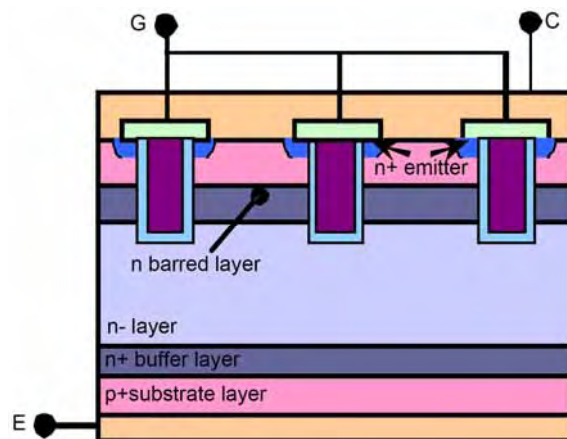
Fig. 3 Structure of full-gate CSTBT

old-generation V Series.

Figure 6 compares the results of thermal simulations for the V1 Series and the old-generation V Series (large package).

The V1 Series uses a smaller chip size than the V Series, and hence has a greater thermal chip resistance. However, the thermal simulation results (input power condition: IGBT 100 W, FWDi 38 W) indicate that the maximum chip temperature $T_{j(max)}$ of the V Series (large package) and the V1 Series (small package) are 153.8°C and 146.1°C at the same input power, respectively. Despite the smaller package size, the temperature rise is reduced.

This thermal design has enabled the V1 Series

chips to be smaller, and the old-generation V Series devices in large packages have been miniaturized into a smaller package. In addition, the V1 Series has the same external dimensions and terminal configuration as the V Series which makes upgrading easy.

3.4 Wire Bonding (Technology to Extend Lifetime)

To meet the needs for extended lifetime, the power cycle lifetime of the V1 Series has been improved by optimizing the wire bonding conditions.

The power cycle curve is shown in Figure 7. The ΔT_j of the V1 Series after 1000k cycles has been improved to Δ60°C from Δ32°C and Δ45°C of the old-generation V Series and L Series, respectively.

4. Conclusion

This article presented the new high-power 2-in-1 IPM V1 Series, which has been developed to meet the needs of the diversifying IPM market for lower power loss, higher capacity and longer lifetime. We believe that the V1 Series will meet market expectations.

We will continue to enhance this high-capacity product lineup as well as develop new IPMs with suitable functionality and performance for various applications, thus contributing to global environmental protection.
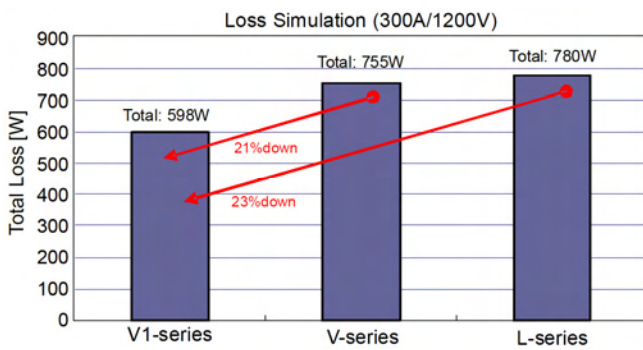

Fig. 4 Calculation result of power loss
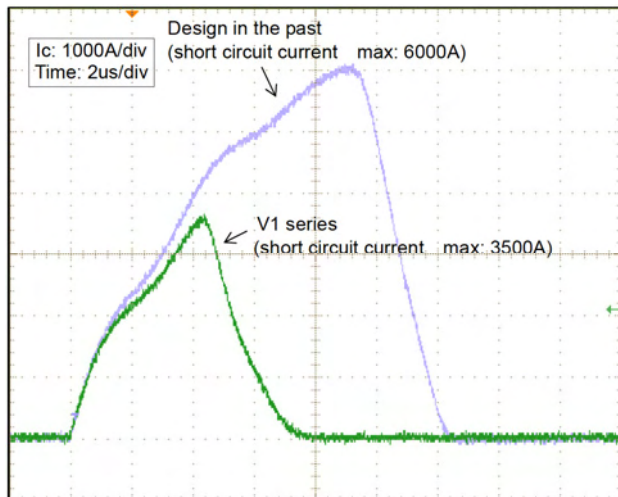(L-series vs V1-series)

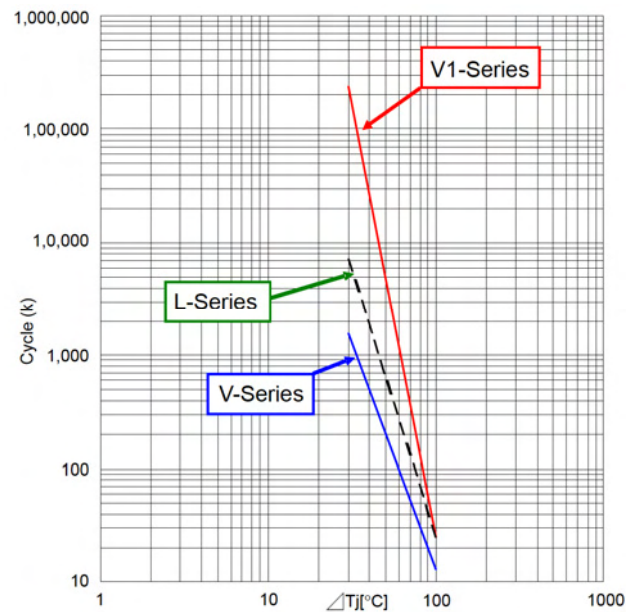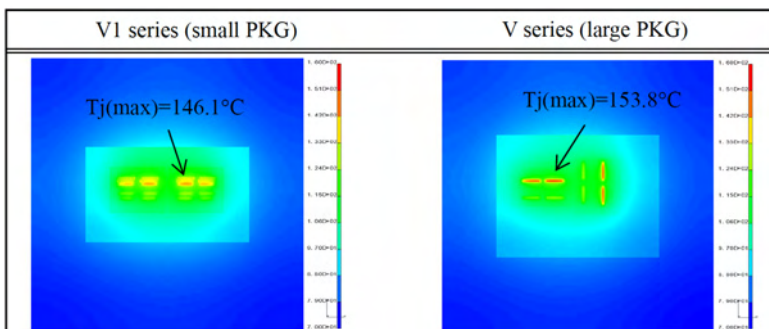Fig. 5 The waveform of short circuit current

Fig. 7 Power cycle curve

Fig. 6 Calculation result of junction temperature

14

Development of 1200V Large DIPIPM™ Ver. 4

Authors: *Tomofumi Tanaka** and *Takuya Shiraishi**

This paper presents the 1200V Large DIPIPM™ Ver. 4 Series, which is compatible with the AC 400V power supply for overseas markets.

The new series has achieved low loss and high heat dissipation by adopting the LPT-CSTBT™ and the insulated high heat dissipation sheet structure. This has enabled a compact product lineup with a wide selection of rated currents, and improved functionality by optimizing the method for detecting short-circuit currents and integrating the module temperature detection capability.

1. Introduction

Mitsubishi Electric′s DIPIPM™ is a transfer molded IPM that has power chips and control IC chips built into the same package, and is widely used for household electric appliances such as air conditioners, refrigerators, and washing machines, as well as for industrial use such as low-power motor drives.

In 2005, to address the rapidly growing demand for energy saving and high-performance applications, Mitsubishi Electric commercialized the 1200V DIPIPM™ Series (5–25 A), the industry′s first transfer molded IPM. Since then, DIPIPMs have helped downsize the inverter boards that drive packaged air conditioners and other industrial motors. This time, for packaged air conditioners and other industrial applications, we have developed and started mass production of the 1200V Large DIPIPM™ Ver. 4 Series (5–35 A), which is more compact and has higher performance than the conventional 1200V DIPIPM™ Series. This article describes the outline, features, internal structure, and built-in functions of the 1200V Large DIPIPM™ Ver. 4 Series.
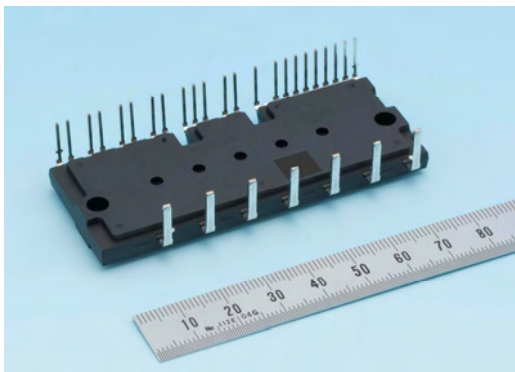

Fig. 1 Outline view of 1200V large DIPIPM™ Ver. 4

2. Outline of the 1200V Large DIPIPM™ Ver. 4 Series

Compared with the conventional 1200V DIPIPM™ Series, the 1200V Large DIPIPM™ Ver. 4 Series has enhanced the lineup of compact products with a wide selection of rated currents. This section describes the features of the 1200V Large DIPIPM™ Ver. 4 Series.

2.1 Low Thermal Resistance

Instead of the conventional mold resin type insulation structure, the new series uses the insulated high heat dissipation sheet structure to reduce the thermal resistance (about 30% reduction from the conventional 1200V DIPIPM™).

2.2 Temperature Detection

A function to detect and output the module temperature as an analog signal is built into the Low Voltage Integrated Circuit (LVIC). This eliminates the need to attach an external thermistor for detecting the module temperature.

2.3 Simplified Short-Circuit Protection Circuit

A new method is employed to detect a short-circuit current by extracting about one thousandth of the emitter current from the power chip. This method enables short-circuit protection without using a high-power shunt resistor, resulting in a significant reduction in the power loss due to the shunt resistor.

2.4 Package Downsizing and Increase in Rated Current

The power loss has been reduced by employing Mitsubishi Electric′s unique 5th-generation LPT-CSTBT™ chip. The thermal resistance has also been reduced by the insulation sheet structure. These improvements have enabled the package to be made about 30% smaller for the same rated current compared to the conventional product. In addition, the product lineup has been enhanced for rated currents of up to 35 A.

3. Circuit Configuration and Performance of 1200V Large DIPIPM™ Ver. 4

The internal circuit of the DIPIPM™ is configured in the conventional manner consisting of six sets of Insulated Gate Bipolar Transistor (IGBT) and Free Wheeling Diode (FWD) chips, and control ICs (HVIC

and LVIC) that control the power chips. Figure 2 shows the internal circuit diagram of the 1200V Large DIPIPM™ Ver. 4 Series.
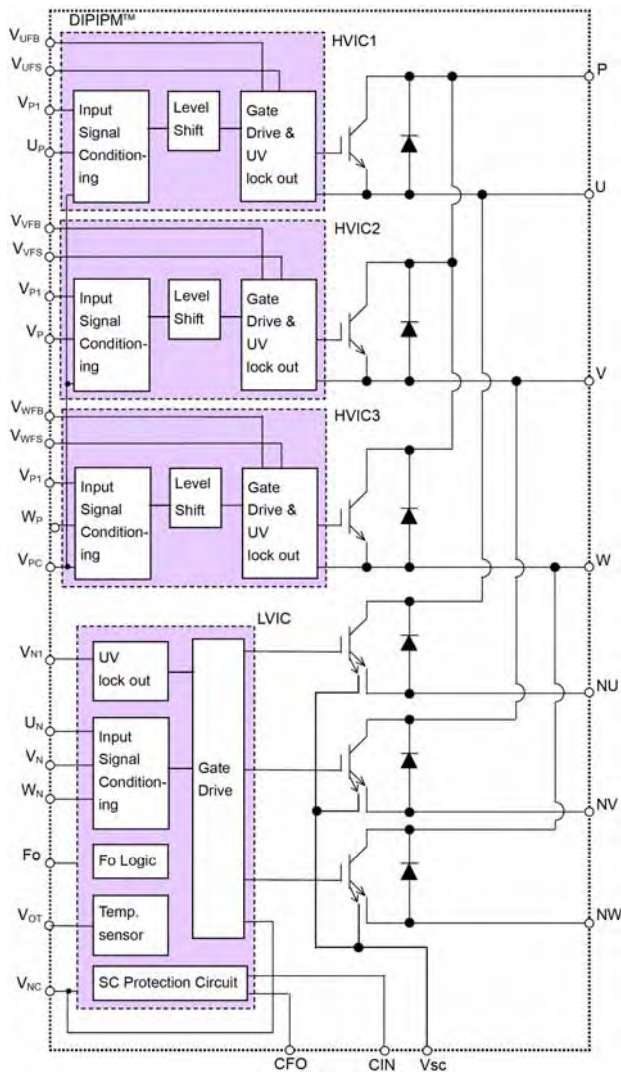

Fig. 2 Internal block diagram of 1200V large DIPIPM™ Ver. 4

3.1 Power Circuit

The three-phase AC output inverter circuit consists of six IGBTs and six FWDs.

3.2 Control ICs

High Voltage Integrated Circuit (HVIC): upper arm IGBT drive circuit, high-voltage level shifter, under-voltage protection circuit for the control power supply (no error output)

Low Voltage Integrated Circuit (LVIC): lower arm IGBT drive circuit, under-voltage protection circuit for the control power supply, LVIC analog temperature output circuit, short-circuit protection circuit (For short-circuit protection, an external current detection resistor is connected to the emitter sense (V_{SC}) terminal of the lower arm IGBT, and when the voltage exceeds the specified threshold voltage, the lower arm IGBTs

are turned off.)

4. Internal Structure of 1200V Large DIPIPM™ Ver. 4

Figure 3 shows cross-sectional diagrams of the 1200V Large DIPIPM™ Ver. 4 and conventional product. The internal structure is configured as follows: power chips, i.e. IGBT and FWD, and control IC chips, i.e. HVIC and LVIC are assembled on a lead frame. Connections are made between the chips using Al wires and Au wires. An aluminum heat sink and insulated heat dissipation sheet are put together and then transfer molded to complete the package.
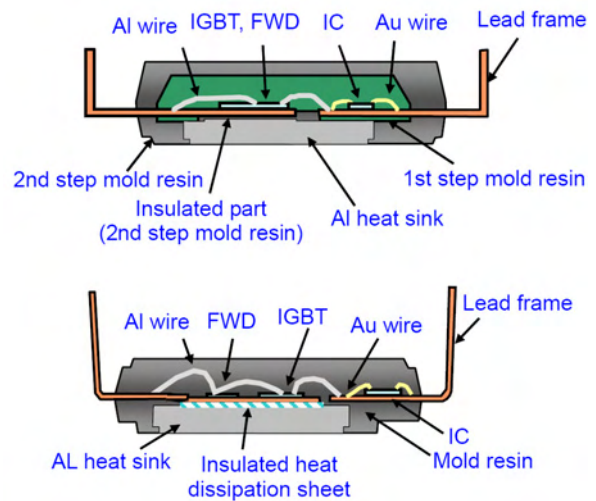

Fig. 3 Internal structure of 1200V large DIPIPM™ Ver. 4

In contrast to the conventional mold resin type insulation method, the greatest feature of the 1200V Large DIPIPM™ Ver. 4 is its insulation structure using an insulated high heat dissipation sheet. This structure eliminates the second step mold process, which was used for insulation between the frame and Al heat sink. With this new structure, the 1200V Large DIPIPM™ Ver. 4 reduces the thermal resistance by about 30% and in a 30% smaller volume than the conventional 1200V DIPIPM™ Series.

5. High Current Capacity and High Performance 1200V Large DIPIPM™ Ver. 4

5.1 High Current Capacity

The 1200V Large DIPIPM™ Ver. 4 Series employs the "LPT-CSTBT™," power chips that Mitsubishi Electric uniquely developed, to reduce the power loss. Figure 4 shows the trade-off relationship between saturation voltage $V_{CE(sat)}$ and turn-off switching loss E_{off} in comparison with the conventional product equipped with planar gate IGBTs.

Thanks to the synergy effect of the power loss reduction and the previously described thermal resistance reduction by using the insulated sheet structure, the

1200V Large DIPIPM™ Ver. 4 Series offers a broader product lineup for rated currents of up to 35 A, in contrast to the previous 1200V DIPIPM™ Series with rated current of up to 25 A. In addition, the smaller package has reduced the footprint by about 30% from the conventional product while the external dimensions remain the same as the already mass-produced 600 V Large DIPIPM™ Ver. 3 and Ver. 4 Series. This enables the same circuit board to be used for different rated voltages, thus improving the efficiency of the circuit board design.
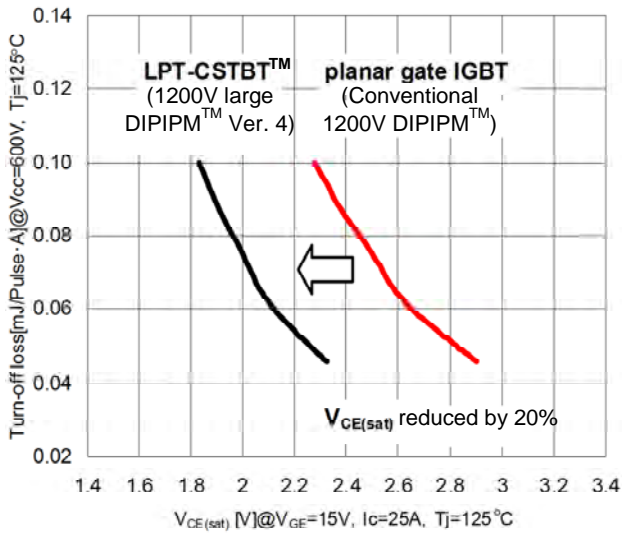

Fig. 4 Trade-off characteristic

5.2 High Performance
(1) Optimization of Short-Circuit Protection Circuit

Conventional short-circuit protection detects the voltage across an external shunt resistor corresponding to the IGBT emitter current and provided protection. In contrast, instead of monitoring an ampere-level large current, the 1200V Large DIPIPM™ Ver. 4 Series has been changed to detect the voltage corresponding to a milliampere-level sense current divided from the emitter current, and to provide protection (Fig. 5). To obtain the sense current, on-chip current sense IGBTs are used for the lower arm power chips. Since the shunt resistor inserted into the emitter current path is no longer needed, an inductance-induced surge voltage across the NU/ NV/ NW terminals and V_{NC} terminal can be suppressed, resulting in increased flexibility of circuit board design. In addition, while the conventional short-circuit protection needs to choose a high wattage type shunt resistor, the sense current detection can reduce the loss, thereby making the circuit board smaller and reducing the cost.

(2) Built-in Temperature Detection Function

Most of the over-temperature protection of the module uses an external thermistor attached near the module's radiation heat sink to detect the temperature. When a thermistor is attached to the heat sink, if the connection between the heat sink and module becomes
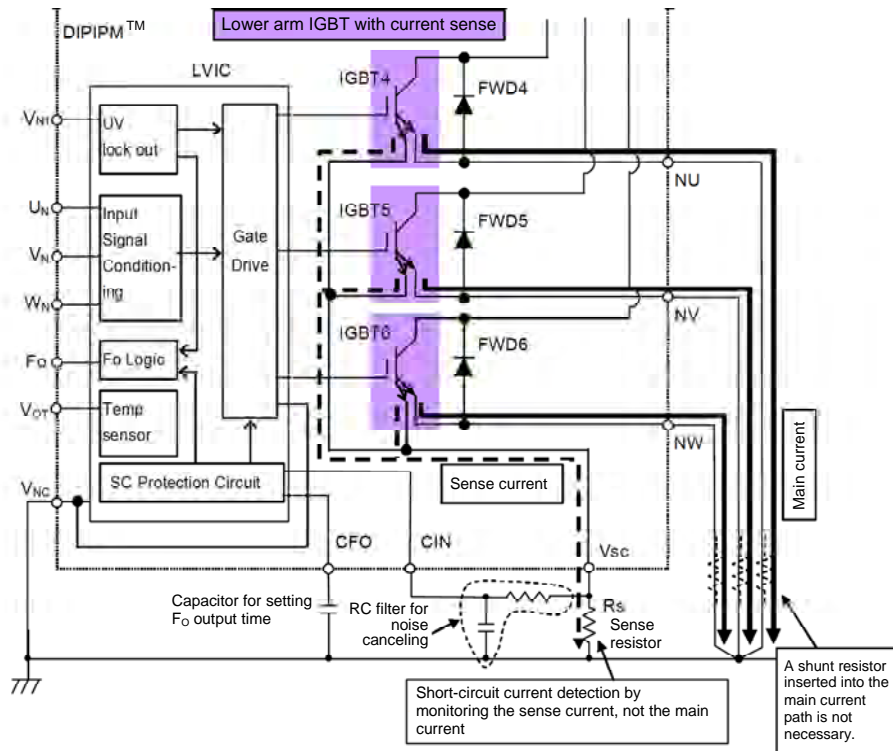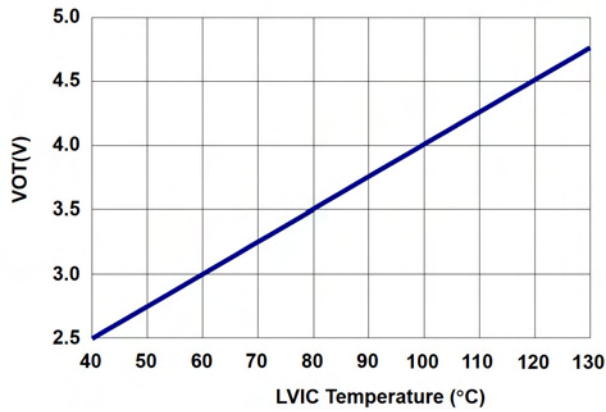

Fig. 5 SC protection circuit

Fig. 6 VOT-LIVC temperature

loose and fails during operation, then the correct module temperature cannot be detected. The temperature detection function used in the new series has a temperature detector built into the control IC (LVIC) and provides an analog voltage output (V_{OT}) (Fig. 6). This function eliminates the need for the external thermistor and reduces the system cost. Furthermore, it ensures the reliability of the temperature information because the signal is directly output from the module.

6. Conclusion

This paper has presented the structure, functions, and features of the newly developed and commercialized 1200V Large DIPIPM™ Ver. 4 Series. We will apply the developed technologies to the same category of products, and will continue to contribute to the inverter market by developing high value-added products taking global environmental protection into account. In addition to developing products for the consumer market, we will also enhance the product lineup to meet the needs of new markets such as solar power generation applications, thus boosting demand for the DIPIPM™.

References

(1) Teruaki Nagahara, et al.: "Deployment of DIP-IPM Ver.4 Series," Mitsubishi Denki Giho, 81, No.5, 349–352 (2007).

(2) Hisashi Kawafuji, et al.: "New 5-35 A/ 1200V Transfer Mold IPM with heat dissipating insulation sheet," PCIM (2008).

MITSUBISHI ELECTRIC CORPORATION